arXiv:cond-mat/0405430v2 [cond-mat.supr-con] 12 Oct 2004

Coherent oscillations in a superconducting multi-level quantum system

J. Claudon[1], F. Balestro[1,2], F. W. J. Hekking[3], and O. Buisson[1]

[1]*Centre de Recherches sur les Très Basses Températures, laboratoire associé à l'Université Joseph Fourier, C.N.R.S., BP 166, 38042 Grenoble-cedex 9, France*

[2]*Department of Nanoscience, Delft University of Technology, Lorentzweg 1, 2628 CJ Delft, The Netherlands*

[3]*Laboratoire de Physique et Modélisation des Milieux Condensés, CNRS & Université Joseph Fourier, BP 166, 38042 Grenoble-cedex 9, France*

Abstract

We have observed coherent oscillations in a multi-level quantum system, formed by a current-biased dc SQUID. These oscillations have been induced by applying resonant microwave pulses of flux. Quantum measurement is performed by a nanosecond flux pulse that projects the final state onto one of two different voltage states of the dc SQUID, which can be read out. The number of quantum states involved in the coherent oscillations increases with increasing microwave power. The dependence of the oscillation frequency on microwave power deviates strongly from the linear regime expected for a two-level system and can be very well explained by a theoretical model taking into account the anharmonicity of the multi-level system.

PACS numbers: 03.67.Lx,05.45.-a,85.25.-j

Up to now, in view of quantum information processing, experiments in solid state devices have concentrated only on the implementation of two-level quantum systems. A variety of quantum circuits based on Josephson junctions [1, 2, 3, 4] and quantum dots [5] have been proposed and realized. Rabi oscillations have been observed showing that the two lowest levels can be manipulated coherently. However, the two-level system is not the only one useful for quantum computation. For instance, multi-level systems are of interest for solving database search problems using quantum algorithms [6], as was demonstrated with Rydberg atoms [7]. Recent theoretical proposals discuss the use of multilevel quantum systems in solid state devices for quantum information processing [8]. In superconducting devices such as a current-biased Josephson junction [9] or a rf SQUID [10], many experiments were performed demonstrating the multi-level quantum nature of these systems. However no experiment has probed coherent behaviour yet. In this letter, we report, to our knowledge, the first observation of coherent oscillations in a multi-level solid-state circuit, based on Josephson junctions. The non-linearity of the Josephson junction plays a crucial role in the quantum dynamics of the device.

Specifically, the quantum system that we study in our experiments is a current-biased dc SQUID. It consists of two Josephson junctions each with critical current I_0 and capacitance C_0. The junctions are embedded in a superconducting loop of inductance L_s, threaded by a flux Φ. Since $L_s I_0 \approx \Phi_0/2\pi$, the phase dynamics of the two junctions can be treated as that of a fictitious particle of mass $m = 2C_0(\Phi_0/2\pi)^2$ moving in a two-dimensional potential, which contains valleys and mountains [11, 12, 13]. Here $\Phi_0 = h/2e$ is the superconducting flux quantum. The local minima are separated from each other by saddle points, where the particle can escape. Along the escape direction, the potential is cubic and can be characterized by a frequency ω_p and a barrier height ΔU, see Fig. 1a. These two quantities depend on the magnetic flux and vanish at the critical current I_c of the SQUID. We assume a complete separation of the variables along the escape direction and the transverse one by neglecting the coupling terms between these two directions. In this approximation, the dynamics of the SQUID's phase ϕ along the escape direction is similar to the dynamics of the phase of a current-biased single Josephson junction [14, 15]. The parameters I_c, ΔU and ω_p are renormalized, thereby taking into account the two-dimensional nature of the potential, as it was demonstrated in [11, 12]. For bias currents $I_b < I_c$, the particle is trapped in a

local minimum and its quantum dynamics is described by

$$\hat{H}_0 = \frac{1}{2}\hbar\omega_p(\hat{P}^2 + \hat{X}^2) - \sigma\hbar\omega_{\rm p}\hat{X}^3, \tag{1}$$

where $\hat{P} = (1/\sqrt{m\hbar\omega_{\rm p}})P$ and $\hat{X} = (\sqrt{m\omega_{\rm p}/\hbar})\phi$ are the reduced momentum and position operators, respectively. Here, P is the operator conjugate to ϕ; $\sigma = 1/(6a)[2(1 - I_{\rm b}/I_{\rm c})]^{-5/8}$ is the relative magnitude of the cubic term compared to the quadratic (harmonic) term. The parameter a is a constant, $a \sim 11$ for our SQUID. For I_b well below I_c, $\Delta U \gg \hbar\omega_p$ and many low-lying quantum states are found near the local minimum. These states, describing the oscillatory motion within the anharmonic (cubic) potential, are denoted $|n\rangle$ for the nth level, with $n = 0, 1, 2, \ldots$. The corresponding energies E_n were calculated in Ref. [15]. Tunnelling through the barrier can be neglected for the lowest-lying states with $n\hbar\omega_{\rm p} \ll \Delta U$. The effect of a time-dependent flux $\Phi(t)$ can be included in Eq. (1) by adding the time-dependent term $\alpha(t)\hbar\omega_{\rm p}\hat{X}$ where $\alpha(t)$is proportional to $\Phi(t)$ [16]. In our experiment, deep quantum states are excited by applying microwave (MW) flux pulses characterized by their frequency ν, amplitude Φ_{MW} and duration ΔT. Starting with $|\Psi(0)\rangle = |0\rangle$, the state evolves with the MW pulse of duration ΔT into a coherent superposition $|\Psi(\Delta T)\rangle = a_0|0\rangle + a_1|1\rangle + \ldots + a_n|n\rangle + \ldots$

Our procedure to perform quantum experiments consists of four successive steps as depicted in Fig. 1b. A bias current I_b is switched on through the SQUID at fixed magnetic flux Φ_{dc} to prepare the circuit at the working point in the initial state $|0\rangle$. The application of a MW flux pulse produces the superposition $|\Psi(\Delta T)\rangle$. Then, a flux pulse of nanosecond duration is applied which brings the system to the measuring point such that the state $|\Psi(\Delta T)\rangle$ is projected onto either the zero or the finite voltage state of the SQUID (Fig. 1c). The result of this quantum measurement can be read out by monitoring the voltage $V_{\rm out}$ across the dc SQUID. Finally, I_b is switched off such that the circuit is reset and the experiment can be repeated to obtain state occupancy.

The aforementioned quantum measurement procedure was discussed theoretically by us in Ref. [16]. Differently from previous experiments which used current bias pulses [2, 4] or MW pulses [3], we implemented a quantum measurement using a large-amplitude flux pulse with nanosecond duration. This flux pulse reduces the SQUID critical current to a value very close to the bias current such that $\Delta U \sim \hbar\omega_p$. Ideally, the pulse with optimal amplitude projects the excited states with $n > 0$ onto the voltage state ($V_{\rm out}$ is twice the

superconducting gap); the ground state $|0\rangle$ is projected onto the zero-voltage state. As the SQUID is hysteretic, the zero and finite voltage states are stable. The efficiency of this one-shot measurement is estimated to be 96% [16]. In the experiment, we use a pulse of $2.5ns$ duration whose $1.5ns$ rise and fall times are long enough to guarantee adiabaticity: transitions between $|0\rangle$ and excited states are estimated to occur with a probability less than 1% for a typical pulse amplitude of $0.06\Phi_0$. The measurement pulse can be applied with a variable delay after the end of the MW pulse. In the measurement procedure, this delay is kept as short as $1.5ns$ to limit relaxation processes. The result of the quantum measurement is obtained by measuring the escape probability P_{esc} repeating the experiment up to about 4000 times.

The measured dc SQUID consists of two aluminum Josephson junctions with $I_0 = 3.028\mu A$ and $C_0 = 0.76pF$, coupled by an inductance $L_s = 98pH$ (see Fig. 1d). The quantum circuit is decoupled from the external classical circuit by long on-chip superconducting thin wires of large total inductance, $L_e = 15nH$, and a parallel capacitor, $C_e = 150pF$. The quantum circuit and the long superconducting wires are realized by e-beam lithography and shadow evaporation. The nominal room temperature microwave signal is guided by 50Ω coax lines and attenuated twice by 20dB (at 1.5K and 30mK, respectively) before reaching the SQUID through a mutual inductance $M_s = 0.7pH$. The MW line is terminated by an inductance estimated to be $L_{MW} = 1nH$. Special care was taken to avoid spurious environmental microwave resonances. The chip is mounted in a shielded copper cavity, cooled down to about 30 mK, whose cut-off frequency is above 20 GHz. Moreover, the thin film capacitor, C_e, close to the chip decouples the microwave signal from the low-frequency bias lines.

The escape probability is first obtained by measurements using long (duration $\Delta t = 50\mu s$) pulses of the bias current I_b. From the dependence of the escape current (defined as the current at which $P_{esc} = 1/2$) on Φ_{dc}, the experimental parameters of the SQUID are extracted [11]. At the maximum value of I_c obtained for $\Phi_{dc}/\Phi_0 = -0.085$, the measured escape rate can be fit by the well-known MQT formula [11, 13] yielding the same SQUID parameters within a 2 % error. This result confirms that the circuit remains in the ground state when only I_b pulses are applied. For other values of Φ_{dc}, the width of the escape probability is larger than the MQT prediction by a factor up to 4 indicating a residual low-frequency flux noise in our sample [4]. This noise reduces the efficiency of our quantum

measurement since it smears the escape probability difference between the ground state and the excited states. In the experiment the nanopulse amplitude is adjusted in order that the escape from $|0\rangle$ is close to 1%. For such a pulse amplitude at $\Phi_{dc}/\Phi_0 = 0.095$, we have estimated that the escape probabilities of the excited states $|1\rangle$, $|2\rangle$, $|3\rangle$ and higher states are about 30 %, 60 %, 90 % and 100% respectively. The sensitivity to flux noise is weakest at the "optimal" point $\Phi_{dc}/\Phi_0 = -0.085$; however, the SQUID's sensitivity to MW and measurement pulses is also weak such that this point cannot be used for accurate measurements.

Spectroscopic measurements were performed by sweeping the frequency of a MW flux pulse of $25ns$ duration in the low power limit. In the inset of Fig. 2 we show the corresponding resonance peak found for P_{esc} versus microwave frequency ν. The resonant frequency ν_{01} depends on I_b as shown in Fig. 2; this dependence can be very well fit by the semiclassical formula for the cubic potential [15]. The parameters extracted from this fit are consistent within 2% error with the parameters extracted from the critical current versus flux dependence or from the MQT measurements at $\Phi_{dc}/\Phi_0 = -0.085$. The large width $\Delta\nu_{01} = 180MHz$ of the resonance peak is consistent with the presence of a residual low-frequency flux noise. Indeed, since the flux through the SQUID fluctuates slowly, the expected resonant frequency changes from one measurement to the other.

We also measured the lifetime of the first excited states, analyzing the decay of the resonance height. Upon increasing the delay time between the end of the MW pulse and the nanosecond dc measurement pulse, the peak height is found to decay with times ranging from 14ns to 60ns. The frequency broadening associated with these lifetimes is estimated to be smaller than 10MHz, i.e., not only less than the width $\Delta\nu_{01}$ of the resonance peak but also less than the detuning frequency associated with the anharmonicity between adjacent levels.

By applying short MW pulses at the resonant frequency $\nu = \nu_{01}$, we induce coherent quantum dynamics. Rabi-like coherent oscillations were observed by measuring escape probability versus MW pulse duration ΔT. In Fig. 3a the escape probability oscillates at a frequency $\Omega_{coh}/2\pi$ of about 300MHz. This frequency increases as the MW flux power increases and ranges from about 100 MHz to 1000 MHz in our experiment. It is always much smaller than the resonance frequency ν_{01}. Oscillation amplitudes as large as 70% were observed for the largest MW power. The oscillations are damped with a characteristic at-

tenuation time of about $12ns$. Similar coherent oscillations have been observed at different working points. The dependence of Ω_{coh} as a function of the MW amplitude Φ_{MW} is shown in Fig. 4. The linear dependence predicted by Rabi theory for a two level system [17] is not observed in our measurements.

To analyse the observed coherent oscillations, we use the following model. We ignore relaxation and decoherence processes and consider the applied MW frequency to be the resonant frequency ν_{01}. If we furthermore assume the MW pulse to couple the eigenstate $|n\rangle$ to its nearest-neighbor levels only, the time-dependent part of the Hamiltonian reads $\alpha(t)\hbar\omega_{\rm p}\hat{X} \approx b\frac{\Phi_{MW}}{\Phi_0}\cos(2\pi\nu_{01}t)\hbar\omega_p\sum_n\sqrt{n/2}[|n\rangle\langle n-1| + |n-1\rangle\langle n|]$, where $b \sim 34$ at the considered working point. As $\Omega_{coh}/2\pi \ll \nu_{01}$, we can use the rotating wave approximation and treat this term non-perturbatively. We obtain the coefficients a_n of the coherent superposition $|\Psi(\Delta T)\rangle$ generated by a pulse of duration ΔT: $a_n = \sum_k \langle e_k|0\rangle\langle n|e_k\rangle e^{-i\lambda_k\Delta T/\hbar}$, where $|e_k\rangle$ and λ_k are the eigenstates and eigenvalues of the Hamiltonian in the rotating frame. The latter are determined numerically and then used to calculate the probabilities $|a_n(\Delta T)|^2$, whose oscillatory time dependence is determined by the frequency differences $\lambda_k - \lambda_j$. At very low MW amplitude ($b\Phi_{MW}/\Phi_0\hbar\omega_p \ll 2E_1 - (E_2 + E_0)$), we obtain the two-level limit: $|\Psi(\Delta T)\rangle$ oscillates between $|0\rangle$ and $|1\rangle$ at the Rabi frequency $\Omega_{coh} = b\omega_p/\sqrt{2}\Phi_{MW}/\Phi_0$ [17]. At larger MW amplitude, an increasing number of states is predicted to participate in the oscillations [18]. As an example, in Fig. 3b the theoretical escape probability is plotted as function of MW pulse duration taking into account the finite efficiency of our measurement. The MW amplitude $\Phi_{MW}/\Phi_0 = 0.002$ was adjusted to fit the measured oscillation frequency. The MW power calibration found from the fit is consistent, within a 30 % error, with the actual applied MW amplitude and with the microwave line and coupling parameters, which were measured independently. The model calculation predicts very large amplitudes, consistent with the experimental results. At $\Delta T = 1.6ns$ the amplitude is close to 100%. In Fig. 3c we indicate the occupancies $|a_n|^2$ of the states $|n\rangle$ that participate in the coherent superposition state at this time. We see that it is concentrated mainly on the states $|4\rangle$, $|5\rangle$ and $|6\rangle$. Finally, the model predicts a slight beating in the oscillations at $\Delta T \sim 20ns$ where the amplitude reaches a minimum. These beating phenomena will not be analyzed in our experiment because they occur at time scales of the order of the above-mentioned attenuation time. For short duration times, the predicted coherent oscillation frequency is given by $\min_{k,l}\{(\lambda_k - \lambda_l)/\hbar\}$. In this limit and using the MW calibration deduced from Fig. 3, we

calculate $\Omega_{coh}/2\pi$ as a function of Φ_{MW}/Φ_0. The result is plotted in Fig.4 together with the experimental one. The perfect agreement between them shows that our model captures the physics of the coherent oscillations.

We reported, to the best of our knowledge, the first observation of coherent oscillations in a multi-level solid-state-based integrated circuit. In our experiment, we have induced coherent superpositions of quantum states which involves many levels using monochromatic microwaves. In order to perform the quantum measurement, we implemented a new measurement procedure based on nanosecond flux pulse through the SQUID. The agreement between our results and the theory proves that the essential physics of our non-linear quantum circuit is well understood.

We thank B. Camarota, F. Faure, Ph. Lafarge, L. Lévy, D. Loss, M. Nunez-Regueiro, B. Pannetier, J. Pekola, and A. Ratchov for useful discussions. This work was supported by ACI and ATIP programs, and by the Institut de Physique de la Matière Condensée. FH acknowledges support from Institut Universitaire de France and the hospitality of NTT Basic Research Laboratories.

---

[1] Yu. Makhlin, G. Schön, and A. Shnirman, Rev. Mod. Phys. **73**, 357 (2001); Y. Nakamura, Yu. A. Pashkin, and J. S. Tsai, Nature **398**, 786 (1999); Y. Yu *et al.*, Science **296**, 889 (2002); T. Yamamoto *et al.*, Nature **425**, 941 (2003).

[2] D. Vion *et al.*, Science **296**, 886 (2002).

[3] J. M. Martinis *et al.*, Phys. Rev. Lett. **89**, 117901 (2002).

[4] I. Chiorescu *et al.*, Science **299**, 1869 (2003).

[5] T. Hayashi *et al.*, Phys. Rev. Lett. **91**, 226804 (2003); R. Hanson *et al.*, Phys. Rev. Lett. **91**, 196802 (2003).

[6] S. Lloyd, Phys. Rev. A **61**, R-010301 (1999).

[7] J. Ahn, T. C. Weinacht, and P.H. Bucksbaum, Science **287**, 463 (2000).

[8] M. N. Leuenberger and D. Loss, Nature **410**, 789 (2001); M. N. Leuenberger *et al.*, Phys. Rev. Lett. **89**, 207601 (2002).

[9] R. V. Voss and R. A. Webb, Phys. Rev. Lett. **47**, 265 (1981); J.M. Martinis, M. H. Devoret, J. Clarke, Phys. Rev. Lett. **55**, 1543 (1985).

[10] J.R. Friedman *et al.*, Nature **406**, 43 (2000).

[11] F. Balestro *et al.*, Phys. Rev. Lett. **91**, 158301 (2003).

[12] V. Lefevre-Seguin *et al.*, Phys. Rev. B **46**, 5507 (1992).

[13] S. Li *et al.*, Phys. Rev. Lett. **89**, 98301 (2002).

[14] J. M. Martinis, M. H. Devoret, and J. Clarke, Phys. Rev. B **35**, 4682 (1987).

[15] A. I. Larkin and Y. N. Ovchinnikov , Sov. Phys. JETP **64**, 185 (1987).

[16] O. Buisson *et al.*, Phys. Rev. Lett. **90**, 238304 (2003).

[17] I. I Rabi, Phys. Rev. **51**, 652 (1937).

[18] M. H. S. Amin, submitted for publication in Phys. Rev. B, cond-mat/0407080.

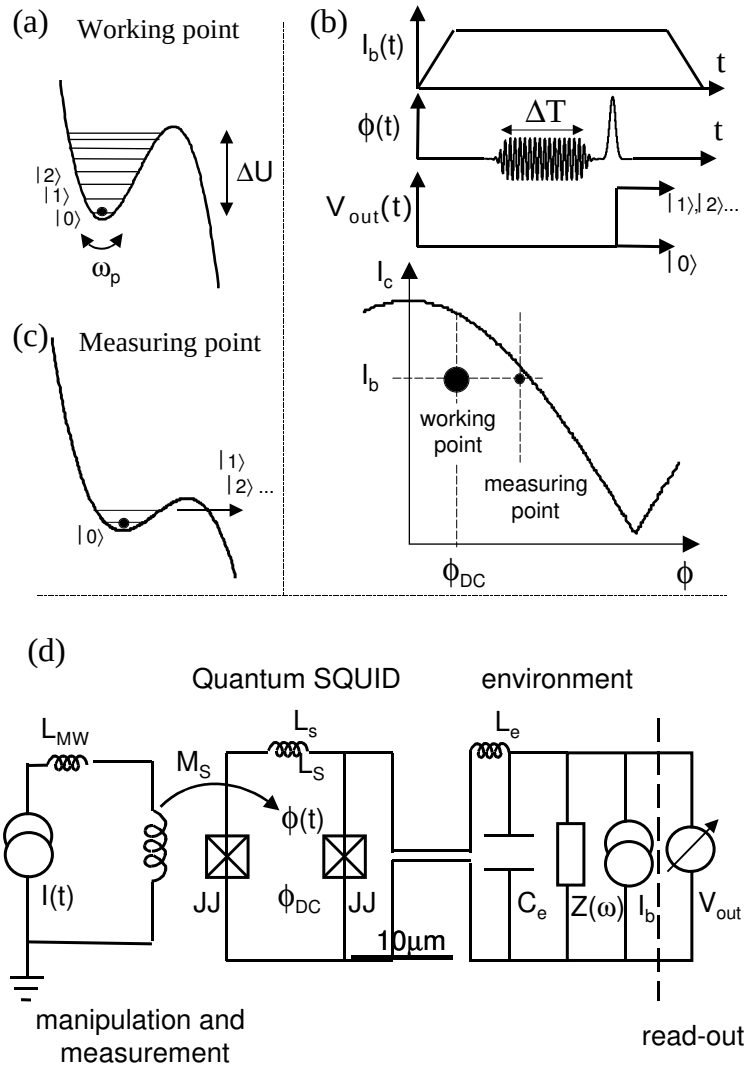


FIG. 1: Quantum experiment and measurement procedure in a dc SQUID. (a) Illustration of the fictitious particle trapped in a deep anharmonic well at the working point. (b) Experimental procedure, as explained in the text. (c) The well at the measuring point: during the nanosecond flux pulse, the particle can escape or remain in the well depending on its quantum state. (d) The dc SQUID consists of two identical Josephson junctions coupled by an inductance L_s. The quantum circuit is decoupled from the environment, symbolized by $Z(\omega)$, by a large inductance L_e and a capacitor C_e; it is coupled by a mutual inductance M_s to the MW pulse or nanosecond pulse through a 50Ω coax line, terminated by an inductance L_{MW}.

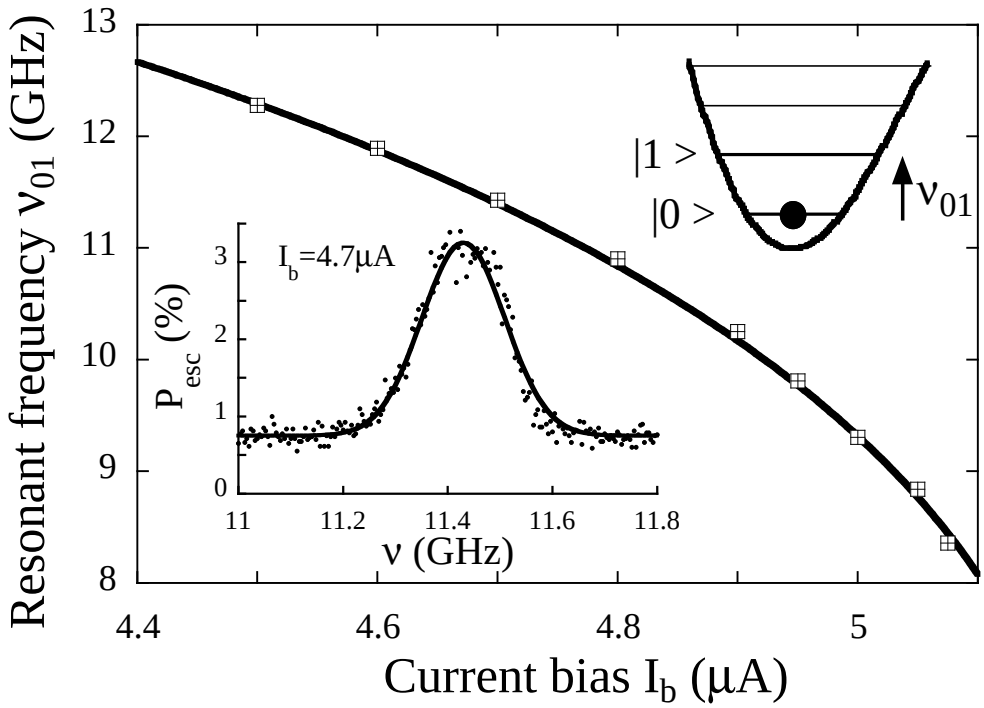


FIG. 2: Resonant transition frequency ν_{01} between states $|0\rangle$ and $|1\rangle$ as function of the bias current at $\Phi_{dc}/\Phi_0 = 0.095$. The experimental dependence of ν_{01} (symbols) on I_b is perfectly described by the semiclassical model [15] (solid line). Spectroscopy is performed by measuring the escape probability P_{esc} versus applied frequency ν (points in inset) at microwave power A=-48dBm where A is the nominal microwave power at room temperature. The fit to a Gaussian (solid line) defines the resonant frequency $\nu_{01} = 11.43GHz$ and the width $\Delta\nu_{01} = 180MHz$.

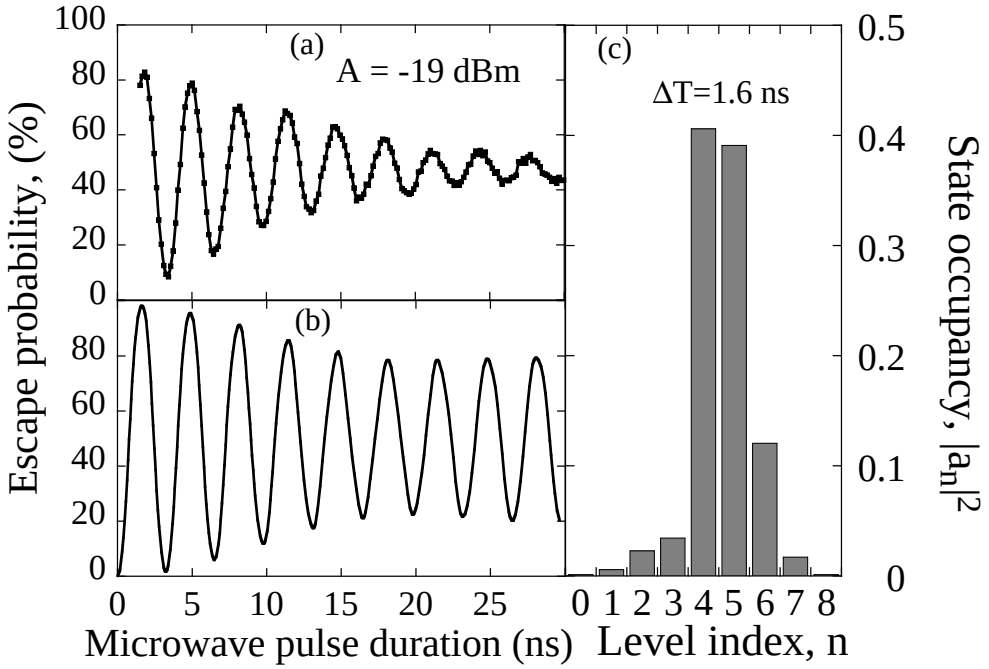


FIG. 3: a) Measured escape probability versus MW pulse duration at the working point, defined by $\Phi_{dc}/\Phi_0 = 0.095$ and $I_b = 4.7\mu A$, with about 15 levels localized in the anharmonic well. b) Predicted escape probability for a MW amplitude $\Phi_{MW}/\Phi_0 = 0.002$. c) a_n coefficients of the state obtained after $1.6ns$ duration of the MW pulse corresponding to the first maximum of the coherent oscillations.

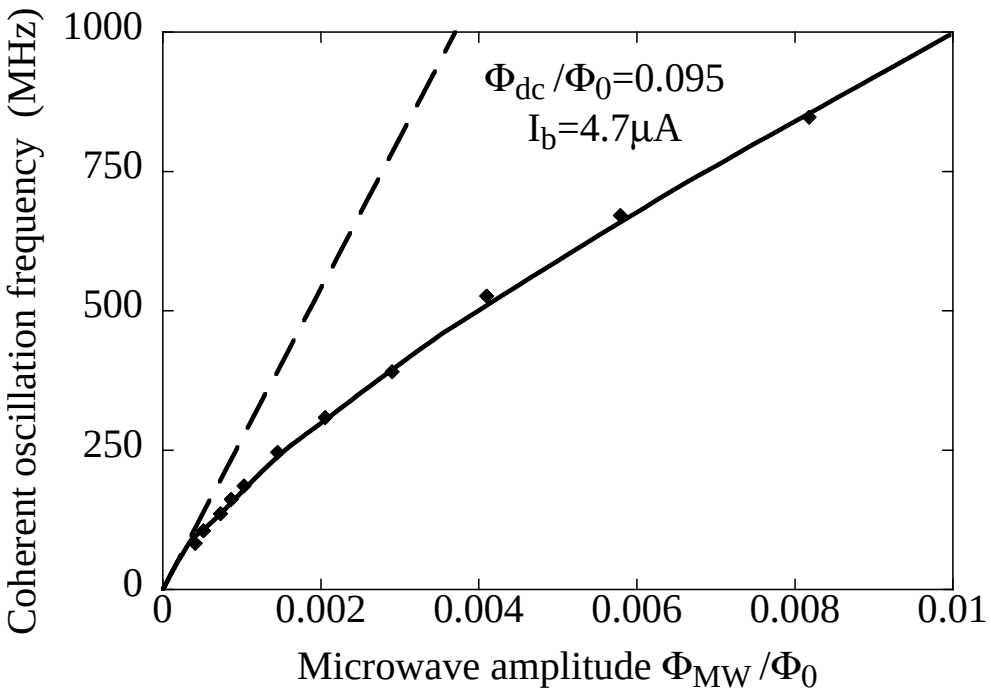


FIG. 4: Frequency of coherent oscillations versus the normalized MW flux amplitude. Dots are experimental results, the solid line the theoretical prediction for a multi-level anharmonic quantum system. Dashed line is the Rabi theory for a two-level system. Experimental calibration of Φ_{MW} is deduced from the fit and is consistent with the estimated Φ_{MW} applied to the set-up.